ISSN 0025-6544, Mechanics of Solids, 2022, Vol. 57, No. 7, pp. 1793–1803. © Allerton Press, Inc., 2022.
Russian Text © The Author(s), 2022, published in Prikladnaya Matematika i Mekhanika, 2022, Vol. 86, No. 2, pp. 276–290.

Damage and Fatigue Fracture of Structural Elements in Various Cyclic Loading Modes

I. S. Nikitin[a],*, N. G. Burago[a,b],, and A. D. Nikitin[a],*****

[a] *Institute for Computer Aided Design, Russian Academy of Sciences, Moscow, Russia*

[b] *Ishlinsky Institute for Problems in Mechanics, Russian Academy of Sciences, Moscow, Russia*

**e-mail: i_nikitin@list.ru*

***e-mail:buragong@yandex.ru*

****e-mail: nikitin_alex@bk.ru*

Received September 30, 2021; revised January 21, 2022; accepted January 27, 2022

Abstract—On the basis of the previously suggested multimode two-criterion model of fatigue fracture, a method is proposed for calculating the origin and development of narrow localized damage zones in structural elements for various modes of cyclic loading. Such narrow zones of damage can be considered as quasi-cracks of two types, corresponding to the mechanism of normal opening and shear fracture.

We consider an important example of a flight loading cycle (high-cycle fatigue) and high-frequency cyclic loading during torsion-bending vibrations of the blades (very-high-cycle fatigue) of an aircraft gas turbine engine compressor disk. The durability of this element of aircraft structures is assessed.

An example of calculating fatigue fracture at high-frequency torsional vibrations of an experimental sample of a certain shape is also considered. For this sample it was possible to reproduce the observed effect of a sharp change in the growth direction and the type of quasi-crack during cyclic loading.

Keywords: fatigue fracture, high-cycle fatigue, very-high-cycle fatigue, multimode model, damage equation, fracture criterion, compressor disk, compressor blades

DOI: 10.3103/S0025654422070135

1. INTRODUCTION

Previously, in [1] a multimode model of the development of fatigue fracture was proposed, which takes into account the bimodality of the fatigue curve under cyclic loading. A review of the principal studies on the theory of fracture in quasi-static, dynamic, and cyclic loading processes [2–11] was also given there. Examples of calculation of several model problems of the development of localized zones of fatigue fracture (quasi-cracks) near structural defects of the material were given and fatigue curves were reproduced for certain types of samples in fatigue experiments for uniaxial tension and torsion.

Then, in [12] and [13], this model was expanded to the case of two different mechanisms of material microfracture, the development of normal opening microcracks, shear microcracks, and, conversely, to considering the two types of macroscopic fracture functions.

Note that the previously proposed working models of the fatigue fracture development by various authors [6–9] describe the modes of low-cycle and high-cycle fatigue.

The proposed model includes a transition to the mode of high-frequency cyclic loading, very-high-cycle fatigue, taking into account the location of the reference points of the right branch of the bimodal fatigue curve (multimode model).

In addition, in models [6–9], numerous coefficients of the evolution damage equation are found purely empirically based on the results of series of tests for complex cyclic loading, which are not always implemented in the very-high-cycle mode. In the proposed model, the coefficients of the kinetic equation for the damage function of the material are obtained using well-known substantiated multiaxial criteria for fatigue failure [14–16]. These coefficients were determined from the condition that the damage development to complete destruction achieved to the corresponding branch of the bimodal fatigue curve. No data besides the shape of the fatigue curve generated from the results of uniaxial reversal tests are required.

Note also that other authors did not explicitly take into account the origin mechanisms of microcracks of various types (normal opening and shear) using the associated fatigue fracture criteria (two-criteria model).

It can be noted that the Chow model [9] takes into account the difference between tension and compression in the accumulation of fatigue fracture by introducing two fracture functions for the degradation of Poisson's ratio and Young's modulus of elasticity. To some extent, this reflects the possibility of developing fatigue fracture by mechanisms of various types.

In this paper, the previously proposed multimode model [12, 13] is used to calculate and evaluate the service life of real structural elements.

A similar practically important problem was already formulated and solved in [17] and [18] for a real structural element of a D30 gas turbine engine compressor, a disk with first-stage blades, for which there were data available on cases of flight accidents in operation [19].

In this case, multiaxial criteria for fatigue fracture were used [20–22], but only in order to indicate the zone of fracture initiation and the corresponding durability based on the elastic solution of the problem on the loading cycle using the appropriate criterion. The kinetics of the further development of fatigue fracture in the structural element was not taken into account.

In this article, we consider practically important examples of calculating the flight loading cycle (low-cycle and high-cycle fatigue) and high-frequency cyclic loading with torsional-flexural vibrations of the blades (very-high-cycle fatigue) of the compressor disk of an aircraft gas turbine engine based on the proposed multi-mode two-criteria model of fracture development under cyclic loading, taking into account the process of initiation and development of narrow localized damage zones (quasi-cracks). For the first time, a comparative analysis of the localization of the initiation and development origin of fatigue quasi-cracks was carried out for various cyclic loading modes and the results were compared to real cases of fracture in the rim of titanium compressor disks in operation.

An example of the calculation of fatigue fracture under high-frequency torsional vibrations of an experimental sample of a certain shape is also considered, in which for the first time it was possible to reproduce the effect of a sharp change in the direction of growth and type of quasi-crack during cyclic loading, confirmed by fractographic studies based on the results of very-high-cycle tests.

This study can be considered as the development of models and methods for the through calculation of the initiation and development of multiple crack-like damage zones (quasi-cracks) of various types under various cyclic loading modes, similar to the methods of through calculation of the development and propagation of shock waves in gas dynamics problems. In both cases, mathematical discontinuities (cracks and shock waves) are spread over a certain (small) number of cells of the computational grid during the calculation, which, nevertheless, makes it possible to quantitatively and qualitatively reflect the main features of the behavior of solutions, taking into account the geometry and type of discontinuities (quasi-cracks).

2. DESCRIPTION OF THE MULTIMODE MODEL OF FATIGUE FAILURE BASED ON DAMAGE THEORY

There are two approaches to study the development of fatigue fracture zones. The first one is based on the classical concepts of linear fracture mechanics and links the conditions for the development of fatigue cracks during an increase in the number of cycles to the amplitudes of stress intensity factors at the crack tip. The fundamental equation was proposed by Paris [23, 24].

The second approach uses the representations of the damage theory, which goes back to [2, 3] and was developed in [4, 5]. In [6–11] it was applied to the problems of cyclic loading and fatigue fracture.

This paper describes a multimode model for the development of fatigue fracture based on the evolution equation for the damage function [1, 12, 13]. It is assumed that in the process of damage to the material (degradation of its properties, in particular, elastic moduli), two mechanisms are at work, the development of normal opening microcracks or shear microcracks. They correspond to the associated criteria of multiaxial fatigue fracture under cyclic uniform loading. Fatigue fracture in the damage development by normal opening microcracks corresponds to the Smith–Watson–Topper (SWT) criterion [14, 15], and fatigue fracture in the damage development by shear microcracks corresponds to the Carpinteri–Spagnoli–Vantadori (CSV) criterion [16].

These and other similar stress-based multiaxial criteria are obtained by generalizing the patterns established for uniaxial loads and described by Wohler-type S–N fatigue curves and Basquin-type relations [25]. In [18], an approach was proposed for extrapolating multiaxial fracture criteria constructed for the

high-cycle mode to the right branches of the fatigue curves in the very-high-cycle mode and using the reference points of each of the branches and the inverse power dependence on number of cycles N to yield to the fatigue limit asymptote. In this paper, this analytical approach was also used to extrapolate the SWT and CSV criteria to the very-high-cycle case.

The following scheme of a multimode (bimodal) fatigue curve with amplitude σ_a is adopted under uniaxial reversal loading. Repeated static loading up to a value of $N_i \sim 10^3$ with an amplitude slightly decreasing from static tensile strength σ_B. Further, the left part of the bimodal fatigue curve describes the low-cycle-high-cycle modes up to values $N \sim 10^7$ reaching fatigue limit σ_u (classical Wohler fatigue curve). These modes on the left branch of the fatigue curve are separated by the magnitude of the loading amplitude, equal to the yield strength of material σ_T. Then, starting from values $N \sim 10^8$, there is a further drop in fatigue strength to new limit value $\tilde{\sigma}_u$ (the right branch of the bimodal fatigue curve in the very-high-cycle mode [19]).

Let us briefly formulate a multimode model of damage development under cyclic loading, all the main theses of which were developed earlier [12].

In presenting it, we restrict ourselves to considering only a part of the left branch of the fatigue curve in the high-cycle mode (stresses do not exceed the yield strength) and, therefore, the problem of determining the stress state within the loading cycle can be solved in the elastic formulation.

In general, as a result of the generalization of Basquin relation [25] $\sigma_a = \sigma_u + \sigma_L N^{-\beta_L}$ to the case of multiaxial loading, the criterion in the high-cycle mode is as follows:

$$\begin{aligned} \sigma_{eq} &= \sigma_u + \sigma_L N^{-\beta_L}, \\ \sigma_L &= 10^{3\beta_L}(\sigma_B - \sigma_u). \end{aligned} \tag{2.1}$$

In these formulas σ_B is the static tensile strength of the material and σ_u is the classical material fatigue limit in reverse cycle (cycle asymmetry factor $R = \sigma_{\min}/\sigma_{\max} = -1$).

Taking into account the approach [18] for extrapolating multiaxial fracture criteria to the very-high-cycle mode by substituting $\sigma_B \to \sigma_u$, $\sigma_u \to \tilde{\sigma}_u$ we obtain multiaxial fatigue fracture criteria in the very-high-cycle mode:

$$\begin{aligned} \sigma_{\text{eq}} &= \tilde{\sigma}_u + \sigma_V N^{-\beta_V}, \\ \sigma_V &= 10^{8\beta_V}(\sigma_u - \tilde{\sigma}_u), \end{aligned} \tag{2.2}$$

where σ_{eq} is the equivalent stress, which generalizes the concept of amplitude under uniaxial cyclic loading to the case of multiaxial loading, and β_L and β_V are indices characterizing the slope of the left and right branches of the bimodal fatigue curve.

Kinetic equation for material damage function ψ, proposed in [1, 12] has the form:

$$\partial\psi/\partial N = B(\sigma, \Delta\sigma)\psi^{\gamma}/(1 - \psi^{1-\gamma}). \tag{2.3}$$

For $\sigma_u + \Delta\sigma_u < \sigma_{eq} < \sigma_B$ (the high-cycle mode, $\Delta\sigma_u = 10^{-5\beta_L}(\sigma_B - \sigma_u)$),

$$B = B_L = 10^{-3}\left[\langle\sigma_{eq} - \sigma_u\rangle/(\sigma_B - \sigma_u)\right]^{1/\beta_L}/(1 - \gamma)/2.$$

For $\tilde{\sigma}_u < \sigma_{eq} \le \sigma_u + \Delta\sigma_u$ (the very-high-cycle mode)

$$B = B_V = 10^{-8}\left[\langle\sigma_{\text{eq}} - \tilde{\sigma}_u\rangle/(\sigma_u - \tilde{\sigma}_u)\right]^{1/\beta_V}/(1 - \gamma)/2.$$

For $\sigma_{eq} \le \tilde{\sigma}_u$ fatigue fracture does not occur and for $\sigma_{eq} \ge \sigma_B$ it happens instantly.

Here and below $\langle f\rangle = fH(f)$, $H(f)$ is the Heaviside function. The value of coefficient $0 < \gamma < 1$ is determined by comparing the calculated and experimentally constructed fatigue curves.

The expressions for effective stresses σ_{eq} are determined by the chosen criteria for total fatigue fracture for two types of damage associated with the development mechanisms of opening or shear microcracks.

The SWT multiaxial criterion describes fatigue fracture with damage development in the form of opening microcracks [1, 15]:

$$\sqrt{\langle\sigma_{1_{\max}}\rangle\Delta\sigma_1/2} = \sigma_u + \sigma_L N^{-\beta_L}, \tag{2.4}$$

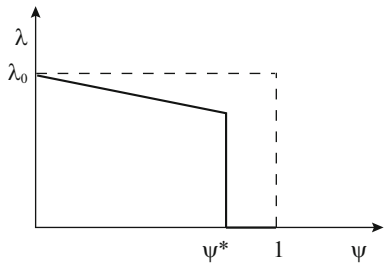

Fig. 1. Dependence of elastic moduli on damage.

where $\sigma_{1_{max}}$ is the maximum value of the principal (tensile) stress and $\Delta\sigma_1$ is its range over the loading cycle.

Therefore, in this case

$$\sigma_{eq} = \sigma^n = \sqrt{\langle\sigma_{1_{max}}\rangle \Delta\sigma_1/2}, \quad \langle\sigma_{1_{max}}\rangle = \sigma_{1_{max}} H(\sigma_{1_{max}}).$$

The multiaxial CSV criterion describes fatigue fracture with damage development in the form of shear microcracks [12, 16]:

$$\sqrt{(\langle\Delta\sigma_n\rangle/2)^2 + 3(\Delta\tau_n/2)^2} = \sigma_u + \sigma_L N^{-\beta_L}. \tag{2.5}$$

Here, $\Delta\tau_n$ is the range of shear stress on the square where it reaches its maximum value (critical square) and $\Delta\sigma_n$ is the range of normal stress on this square.

Therefore, in this case

$$\sigma_{eq} = \sigma^\tau = \sqrt{(\langle\Delta\sigma_n\rangle/2)^2 + 3(\Delta\tau_n/2)^2}, \quad \langle\Delta\sigma_n\rangle = \Delta\sigma_n H(\sigma_{n_{max}}).$$

The initiation of a damage zone in a material particle with an increase in the number of loading cycles due to nonzero coefficient B appearing in the kinetic equation determines the further type of damage in this particle according to the mechanism of development of normal opening microcracks $\max(\sigma^n, \sigma^\tau) = \sigma^n$ or according to the mechanism of development of shear microcracks at $\max(\sigma^n, \sigma^\tau) = \sigma^\tau$.

The development of damage in a material particle leads to an effective decrease in the elastic moduli, generally according to a nonlinear law, and in the proposed version of the model, according to a piecewise linear law of the following form:

material degradation at $\psi < \psi_*$

$$\lambda(\psi) = \lambda_0(1 - \kappa\psi), \quad \mu(\psi) = \mu_0(1 - \kappa\psi) \tag{2.6}$$

complete fracture at $\psi_* \le \psi \le 1$

$$\lambda = 0, \quad \mu = 0.$$

Here, $\psi_* \gtrsim 1$ is the critical damage value at which the destruction is complete (Fig. 1).

3. NUMERICAL METHOD FOR CALCULATING DAMAGE

The numerical method for calculating damage zones consists in step-by-step (by loading cycles) calculation of the elastic stress state of a material sample or structural element, in parallel with the numerical solution of the nonlinear equation for damage (2.3) and the correction of the elastic moduli of the medium in areas where the damage function is non-zero (2.6). Such areas become additional developing stress concentrators, and localized zones of complete fracture in the above sense are treated as quasi-cracks. The quasi-cracks reaching the boundaries of the loaded body is considered as its total destruction on a macro level.

To integrate Eq. (2.3), we used an approximation of the damage function at the kth node of the computational grid for given discrete values ψ_k^n at time moments N^n and sought values of ψ_k^{n+1} at time moments N^{n+1}.

A scheme for approximating the nonlinear equation for damage was applied, based on step-by-step analytical integration of the kinetic equation at a fixed stress state from the previous calculation step over loading cycles:

$$\left[\psi^{1-\gamma}/(1-\gamma) - \psi^{2(1-\gamma)}/2/(1-\gamma)\right]\Big|_{\psi_k^n}^{\psi_k^{n+1}} = B^n N\Big|_{N^n}^{N^{n+1}},$$

where k is the number of the node of the computational grid and n is the number of the step in terms of the number of cycles. Such an algorithm corresponds to an explicit-implicit scheme (explicit in the calculation of the stress field and implicit in the calculation of the damage function).

The formula for the damage function on the top layer has form:

$$\psi_k^{n+1} = \left(1 - \sqrt{\left(1 - (\psi_k^n)^{1-\gamma}\right)^2 - 2(1-\gamma)B^n \Delta N^n}\right)^{1/(1-\gamma)} \tag{3.1}$$

and the calculation step for the number of cycles is determined as follows:

$$\Delta\tilde{N}_k^n = \left[\psi^{1-\gamma}/(1-\gamma) - \psi^{2(1-\gamma)}/2/(1-\gamma)\right]\Big|_{\psi_k^n}^{1} \Big/ B^n,$$
$$\Delta N^n = \min_k 0.5\Delta\tilde{N}_k^n. \tag{3.2}$$

In the numerical implementation, Poisson's ratio of the material does not change, and Young's modulus of elasticity decreases with an increasing damage function according to the law that includes its small residual value in the state of total destruction, equal (for definiteness) to a thousandth of the original value:

$$E_k^{n+1} = E_0\left(1 - \kappa\psi_k^{n+1}\right)\left(H\left(\psi_* - \psi_k^{n+1}\right) + 0.001\right). \tag{3.3}$$

Such an algorithm makes it possible to carry out a continuous calculation of fatigue fracture with the formation and propagation of quasi-cracks without explicitly selecting them and on a fixed grid.

Elastic calculations of the loading cycle in the quasi-static mode (high-cycle) and in the dynamic mode (high-frequency oscillations, very-high-cycle) were performed using the ASTRA and ANSYS software packages. The ASTRA package is a highly efficient software package developed on the basis of a matrix-free FEM variant for solving a wide range of problems in continuum mechanics [26, 27].

The packages were supplemented with code for calculating the kinetics of fatigue fracture and changing the elastic moduli in accordance with the above algorithm.

4. CALCULATION EXAMPLES

4.1. Calculation of the Gas Turbine Engine Structural Element

Using the proposed model and computational algorithm, the initiation and development of a quasi-crack was calculated under two modes of cyclic loading for an important element of the aircraft structure, the disk and blades of the first stage of the D30KU gas turbine engine compressor.

A characteristic view of a destroyed disk and the origin area in the contact zone of the disk and blade is shown in Fig. 2 [28]. Using the example of real destruction of one of the disks in operation, we note the need for a multifactorial multicriteria approach to assessing the resource of titanium compressor disks.

The geometry of the disk sector and blade with shrouds is shown in Fig. 3 and their elastic stress-strain state was previously calculated in [17, 18] without taking into account the development of the damage process.

The aluminum blade is inserted into the dovetail notch of the titanium disk and is additionally fastened to it with a steel cylindrical pin (Fig. 3b). The contact surfaces of the disc and blade allow slippage with friction coefficient q, and the no-slip condition is fulfilled at the contact boundary with the pin.

The mathematical formulation of the corresponding problem of elasticity theory with nonlinear contact conditions is given in [17, 18].

In the first cyclic process of the flight loading cycle "take-off–flight-landing" (pulsating cycle, asymmetry coefficient $R = 0$, high-cycle mode) the sector of the disc with the blade is loaded by centrifugal forces during rotation with angular velocity ω and aerodynamic pressure on the blade estimated by the hypothesis of an isolated profile, for the flow around each section of the blade at a variable angle of attack [17, 18].

(a) (b)

Fig. 2. (a) Origin area in the contact zone of the disc and blade; (b) view of the destroyed disk.

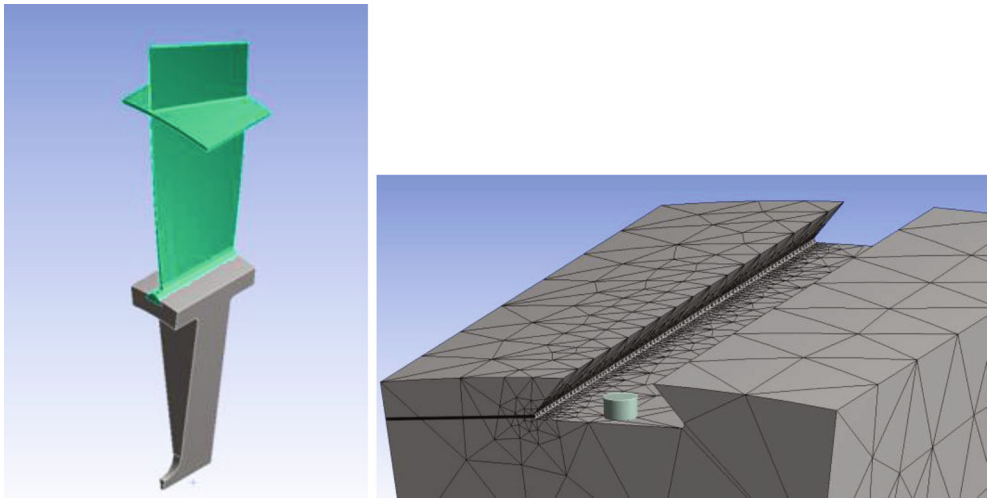

(a) (b)

Fig. 3. (a) Disk sector and blade, (b) stress concentration zone in the vicinity of the dovetail notch.

Figure 3b shows the finite element mesh for calculating a single sector with a blade. The mesh is significantly finer in the vicinity of the expected damage zone. The total number of elements does not exceed 1 million.

The following calculation parameters were adopted: angular rotation velocity $\omega = 419$ rad/s (4000 rpm), freestream velocity head $\rho v_\infty^2/2 = 26000$ N/m^2, which corresponds to the flow velocity of 200 m/s at density 1.3 kg/m^3. The material properties were taken as follows: disc (titanium alloy): Young's modulus $E = 116$ GPa, Poisson's ratio $\nu = 0.32$, density $\rho = 4370$ kg/m^3; blade (aluminum alloy): $E = 69$ GPa, $\nu = 0.33$, $\rho = 2700$ kg/m^3; pin (steel): $E = 207$ GPa, $\nu = 0.27$, $\rho = 7860$ kg/m^3, coefficient of friction $q = 0.1$. Strength and fatigue parameters of titanium alloy are equal: tensile strength $\sigma_B = 1160$ MPa, classical fatigue limit $\sigma_u = 340$ MPa, $\tilde{\sigma}_u = 250$ MPa, $\beta_L = 0.31$, $\beta_V = 0.27$. The parameters of the damage equation according to the results of numerical experiments and comparison of calculated and experimental fatigue curves [12, 13] are chosen as follows: $\gamma = 0.5$, $\kappa = 0.5$, $\psi_* = 0.98$.

The results of calculations of the development of damage in the disk during the flight loading cycle are shown in Figs. 4 and 5. These figures show the distribution of effective stresses in two sections: the cross section of the disk passing through the point of origin of damage and the longitudinal section passing from the left corner of the dovetail notch to the side surface of the disk sector (this section is marked in Fig. 3b by the solid black line).

The maximum effective stresses at the beginning of the cyclic process are 913 MPa according to the SWT criterion and 615 MPa according to the CSV criterion. Therefore, the mechanism of development

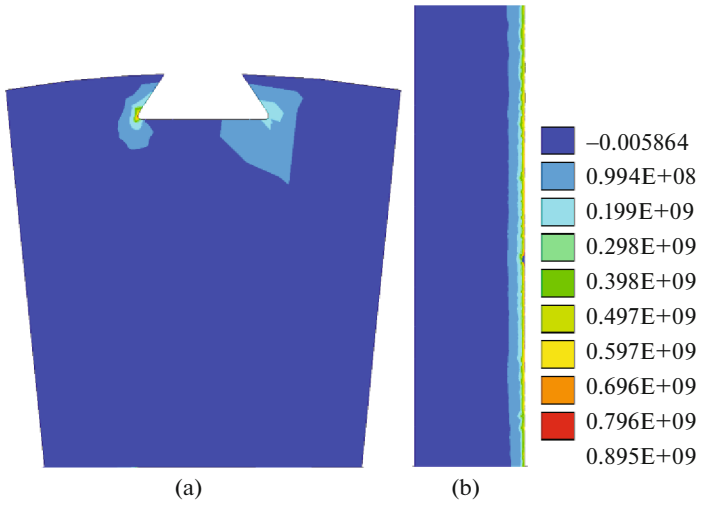

Fig. 4. Distribution of effective stresses in the disk in the contact area of the blade attachment, high-cycle loading: (a) cross-sectional view, (b) longitudinal sectional view at the moment of quasi-crack initiation, $N = 5.2 \times 10^4$.

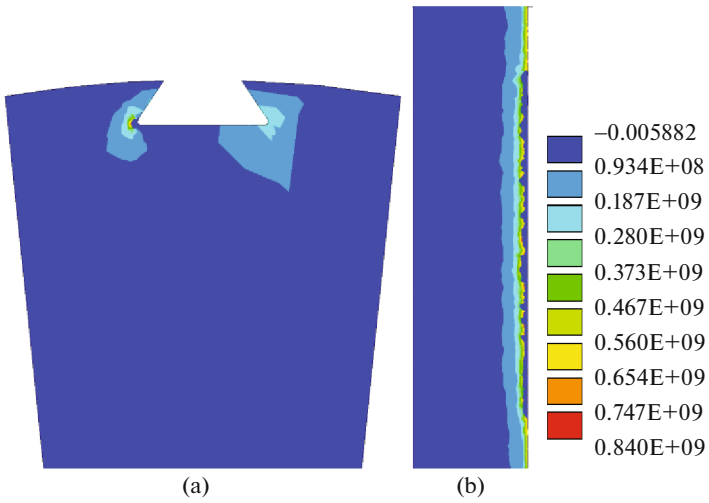

Fig. 5. Distribution of effective stresses in the disc in the contact area of the blade attachment, high-cycle loading: (a) cross-sectional view, (b) longitudinal sectional view with further growth of the quasi-crack, $N = 2.0 \times 10^5$.

of opening microcracks is at work. A quasi-crack appears after $N = 5.2 \times 10^4$ cycles (Fig. 4). The origin zone is in the middle of the left corner of the dovetail (a small black dot on the right edge of the section shown in Fig. 4b). The emergence of a quasi-crack on the end surface of the disk occurs approximately at the number of cycles $N = 2.0 \times 10^5$ (Fig. 5). Thus, it is possible to describe the process of damage development, which, in contrast to the standard schemes for calculating durability by multiaxial criteria of fatigue fracture and the origin time of the initial defect, makes it possible to trace the duration and geometry of the development of quasi-cracks of one type or another.

In the second cyclic process, we calculated the observed high-frequency flexural-torsional vibrations of the blade caused by axial displacements of the ends of the shroud shelves of amplitude $\Delta u \sim 0.5$ mm (reverse cycle, asymmetry factor $R = -1$, very-high-cycle mode). These prolonged vibrations of the stress field in the contact zone of the disk and blades can also lead to the initiation and development of damage (the alternative mechanism of destruction [19]).

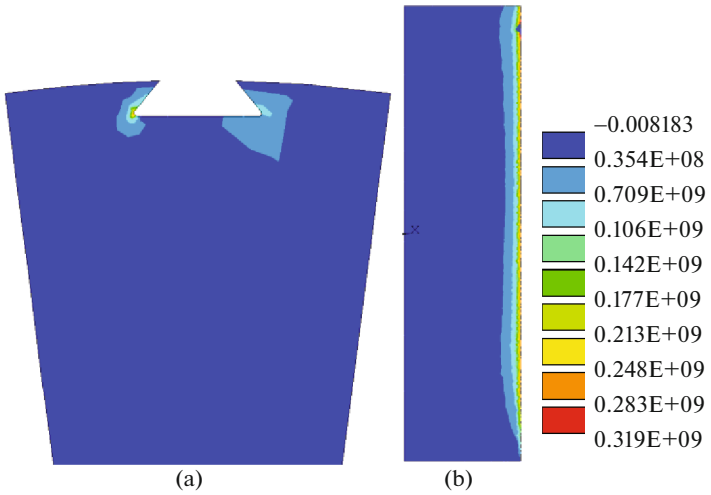

Fig. 6. Distribution of effective stresses in the disk in the contact area of the blade attachment, very-high-cycle loading: (a) cross-sectional view, (b) longitudinal sectional view at the moment of quasi-crack initiation, $N = 7.3\times10^{10}$.

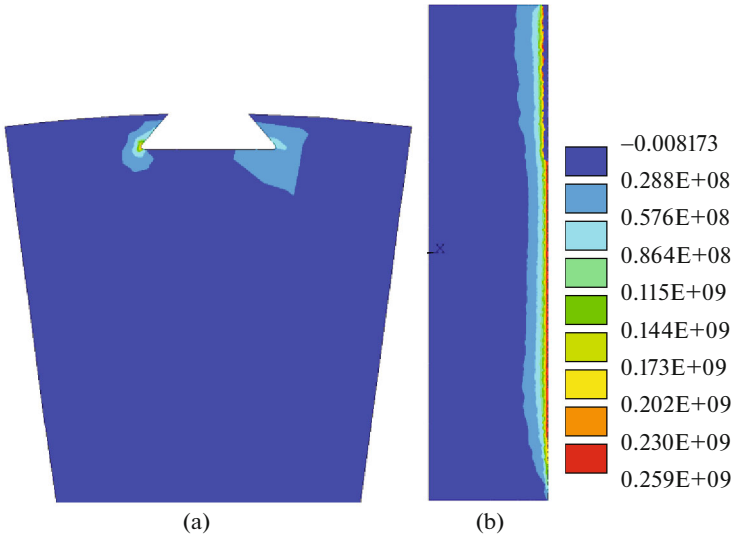

Fig. 7. Distribution of effective stresses in the disc in the contact area of the blade attachment, very-high-cycle loading: (a) cross-sectional view, (b) longitudinal sectional view with further growth of the quasi-crack, $N = 1.5\times10^{11}$.

Figures 6 and 7 show the results of the calculation for bending-torsional vibrations of the blade with a frequency of 1000 Hz, caused by axial vibrations of the shroud ends of amplitude $\Delta u = 0.55$ mm. The origin zone is in the dovetail zone far from the pin and the initiation starts at number of cycles $N = 7.3\times10^{10}$ (small black dot on the right edge of the section shown in Fig. 6b). This characteristic location of the initiation area is also observed in the case of real fatigue fracture of this structural element (Fig. 2a). The quasi-crack grows, reaches the end of the disk, and becomes observable from the outside at $N = 1.5\times10^{11}$ (Fig. 7), so the development process takes a rather long time in this mode as well: the time can be estimated using the proposed kinetic damage model.

It is possible to estimate the real time of quasi-crack initiation in each of the modes. Assuming an average flight cycle is approximately 3 h, in the high-cycle mode $T_1 = 5.2\times10^4\times3$ h ~ 1.6×10^5 h. In the very-high-cycle mode at an oscillation frequency of 1000 Hz, $T_2 = 7.3\times10^{10}\times0.001$ s ~ 2.0×10^4 h Thus, these

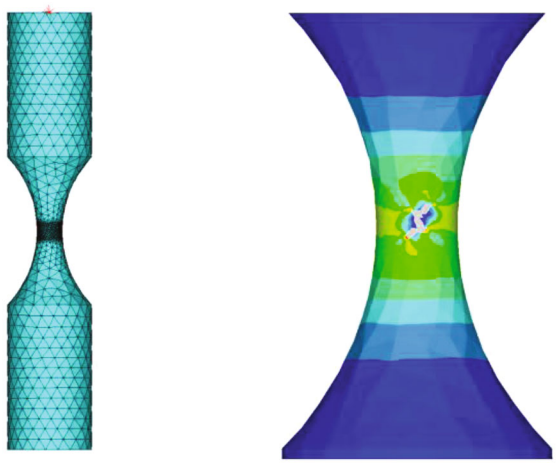

Fig. 8. (a) Finite element mesh in the corset sample, (b) result of calculation of a zigzag quasi-crack.

estimates, as well as the specific localization of the damage initiation area, show that the origin of the initial microcrack is more likely by the very-high-cycle mechanism.

Calculation of high-frequency torsional vibrations of an hourglass-shaped sample.

In this study we also carried out numerical modeling of experiments on the development of a very-high-cycle crack and fatigue fracture during high-frequency torsion of titanium alloy samples.

The tests were performed using a direct piezoelectric fatigue torsion machine [29]. The frequency of reverse oscillations was 20 kHz. The tests were designed to provide fatigue life for over 10^7 cycles. Sample geometry was an hourglass with a smooth section (Fig. 8a). The torsion test material was a titanium alloy with the following characteristics: Young's modulus $E = 115$ GPa, density $\rho = 4500$ kg/m^3, Poisson's ratio $\nu = 0.3$, classical fatigue limit $\sigma_u = 440$ MPa, very-high-cycle fatigue limit $\tilde{\sigma}_u = 380$ MPa. The amplitude of torsional vibrations was 0.01 rad.

The main goal of numerical modeling is to study the trajectory and type of a quasi-crack. Figure 8b shows an example of a crack trajectory developing on the lateral surface of a sample.

The results of calculating the damage zone in the corset-type sample in the very-high-cycle mode are shown in Figs. 8b and 9a. A characteristic view of a quasi-crack is shown in Fig. 8b (grey). The enlarged image of the calculation result shows a zigzag crack path typical for torsional loading (Fig. 9a). It was found that at the initial stage of damage development, the elements were destroyed according to the shear mechanism. This corresponds to a vertical quasi-crack along the sample axis (Fig. 9a). After that, the normal opening quasi-cracks became the dominant fracture mechanism. This period corresponds to the inclined section of the quasi-crack trajectory (Fig. 9a).

Comparison of numerical simulation results with experimental data [29] (Fig. 9b) shows a qualitative match of the trajectories and types of cracks studied by the fractographic method at similar moments of the cyclic loading process. This is a non-trivial result, since it was obtained via the proposed mathematical model using a uniform computational algorithm as a result of an end-to-end calculation. Thus, the model demonstrates the possibility of calculating the initiation and development of various types of quasi-cracks in a single cyclic process, as well as the possibility of a sharp change in the trajectory and damage mechanism in good agreement with the experimental results under multiaxial loading.

The developed multimode model and numerical method make it possible to carry out an through calculation of the development of damage zones and crack-like zones of fatigue fracture of structural elements and experimental samples without explicitly identifying cracks in their classical sense, as well as to evaluate the durability of structural elements from the appearance of the first centers to macrofailure in various modes of fatigue fracture.

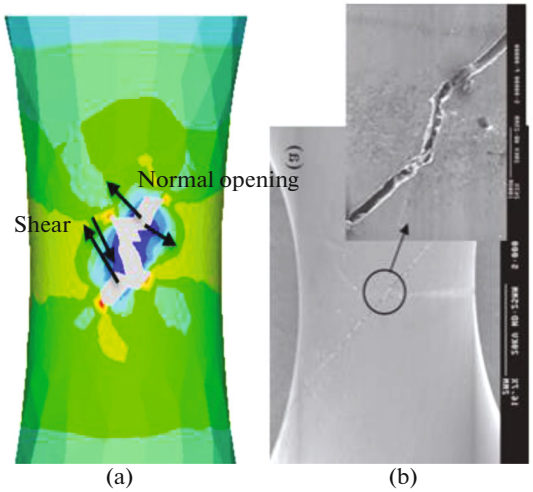

Fig. 9. (a) Change of quasi-crack type in numerical calculation; (b) observed crack trajectory in torsion tests.

CONCLUSIONS

A multimode two-criteria kinetic model of damage development under cyclic loading is proposed to describe the development of the fatigue fracture process. The well-known criteria of multiaxial fatigue fracture are used to determine the coefficients of the kinetic damage equation: the SWT criterion, which includes the development mechanism of normal opening microcracks and the CSV criterion, which includes the development mechanism of shear microcracks.

A uniform numerical method has been developed and an example of calculating the development of crack-like zones of damage and fatigue failure is given for an aircraft gas turbine engine compressor disk in a flight loading cycle (high-cycle fatigue) and at high-frequency torsional-flexural vibrations of blades (very-high-cycle fatigue). An estimate is given for the durability of the considered structural element.

The results of the calculation of fatigue fracture under high-frequency torsional vibrations of an hourglass-shaped experimental sample are also presented. For this case it was possible to reproduce the observed effect of a sharp change in the direction of growth and type of quasi-crack during cyclic loading.

The results obtained qualitatively and quantitatively agree with the data of fractographic studies of cases of fatigue fracture of compressor disks in operation and experiments on high-frequency torsional vibrations of samples in the very-high-cycle mode.

FUNDING

The study was carried out within the framework of the State Contract of the ICAD RAS.

REFERENCES

1. N. G. Burago, I. S. Nikitin, and A. B. Zhuravlev, "Models of multiaxial fatigue fracture and service life estimation of structural elements," Mech. Solids **46** (6), 828–838 (2011). https://doi.org/10.3103/S0025654411060033
2. L. M. Kachanov, "Fracture time under creeping," Izv. Akad. Nauk SSSR, Otd. Tekh. Nauk **8**, 26–31 (1958).
3. J. N. Rabotnov, "Long-term friction mechanism," in *Strength Problems for Materials and Structures* (USSR Acad. Sci., 1959), pp. 5–7 [in Russian].
4. J. Lemaitre and J. L. Chaboche, *Mechanics of Solid Materials* (Univ. Press, Cambridge, 1994).
5. N. G. Burago, I. S. Nikitin, A. D. Nikitin, and B. A. Stratula, "Algorithms for calculation damage processes," Fratt. Integr. Strutturale **49**, 212–224 (2019).
6. A. K. Marmi, A. M. Habraken, and L. Duchene, "Multiaxial fatigue damage modeling at macro scale of $Ti_6A_{l4}V$ alloy," Int. J. Fatigue **31**, 2031–2040 (2009).
7. J. L. Chaboche and P. M. Lesne, "A non-linear continuous fatigue damage model," Fatigue Fract. Eng. Mater. Struct. **11**, 1–17 (1988).
8. R. H. Peerlings, W. A. Brekelmans, R. de Borst, and M. G. Geers, "Gradient-enhanced damage modelling of high-cycle fatigue," Int. J. Num. Method Eng. **49**, 1547–1569 (2000).

9. C. L. Chow and Y. Wei, "Constitutive modeling of material damage for fatigue failure prediction," Int. J. Damage Mech. **8** (4), 355–375 (1999).
10. O. Plekhov and O. Naimark, et al., "The study of a defect evolution in iron under fatigue loading in gigacycle fatigue regime," Fratt. Integr. Strutturale **10** (35), 414–423 (2016).
11. V. N. Shlyannikov, "Creep-fatigue crack growth rate prediction based on fracture damage zones models," Eng. Fract. Mech. **214**, 449–463 (2019).
12. I. S. Nikitin, N. G. Burago, A. D. Nikitin, and B. A. Stratula, "On kinetic model of damage development," Proc. Struct. Integr. **28**, 2032–2042 (2020).
13. I. S. Nikitin, A. D. Nikitin, and B. A. Stratula, "Study on the resonant torsion vibration in hourglass specimens under VHCF loading," J. Phys.: Conf. Ser. **1945** (1), 012043 (2021).
14. R. N. Smith, P. Watson, and T. H. Topper, "A stress-strain parameter for the fatigue of metals," J. Mater. **5** (4), 767–778 (1970).
15. N. Gates and A. Fatemi, "Multiaxial variable amplitude fatigue life analysis including notch effects," Int. J. Fatigue **91**, 337–351 (2016).
16. A. Carpinteri, A. Spagnoli, and S. Vantadori, "Multiaxial assessment using a simplified critical plane based criterion," Int. J. Fatigue **33**, 969–976 (2011).
17. N. G. Bourago, A. B. Zhuravlev, and I. S. Nikitin, "Models of multiaxial fatigue fracture and service life estimation of structural elements," Mech. Solids **46** (6), 828–839 (2011). https://doi.org/10.3103/S0025654411060033
18. N. G. Burago and I. S. Nikitin, "Multiaxial fatigue criteria and durability of titanium compressor disks in low- and giga- cycle fatigue modes," in *Mathematical Modeling and Optimization of Complex Structures* (Springer, Heidelberg, 2016), pp. 117–130.
19. A. A. Shanyavskii, *Modelling of Metal Fatigue Fracture* (Monografia, Ufa, 2007) [in Russian].
20. G. Sines, "Behavior of metals under complex static and alternating stresses," in *Metal Fatigue* (McGraw-Hill, 1959), pp. 145–169.
21. B. Crossland, "Effect of large hydrostatic pressures on torsional fatigue strength of an alloy steel," in *Proc. Int. Conf. on Fatigue of Metals* (London, 1956), pp. 138–149.
22. W. Findley, "A theory for the effect of mean stress on fatigue of metals under combined torsion and axial load or bending," J. Eng. Ind. **81** (4), 301–305 (1959).
23. P. C. Paris and F. Erdogan, "A critical analysis of crack propagation laws," J. Basic Eng. **85**, 528–533 (1963).
24. J. A. Collins, *Failure of Materials in Mechanical Design: Analysis, Prediction, Prevention* (Wiley, New York, 1993).
25. O. H. Basquin, "The exponential law of endurance tests," Proc. Am. Soc. Testing Mater. **10**, 625–630 (1910).
26. N. G. Burago, I. S. Nikitin, and V. L. Yakushev, "Hybrid numerical method with adaptive overlapping meshes for solving nonstationary problems in continuum mechanics," Comput. Math. Math. Phys. **56** (6), 1065–1074 (2016).
27. N. G. Burago and I. S. Nikitin, "Algorithms of through calculation for damage processes," Komp'yut. Issled. Model. **10** (5), 645–666 (2018).
28. A. A. Shanyavskii, "Safety exploitation for disks and low-pressure compressor's stages of D-30KU engine according to fatigue crack growth," Probl. Bezop. Poletov, No. 1, 20–48 (2011).
29. A. Nikitin, C. Bathias, and T. Palin-Luc, "A new piezoelectric fatigue testing machine in pure torsion for ultrasonic fatigue tests: application to forged and extruded titanium alloys," Fatigue Fract. Eng. Mater. Struct. **38** (11), 1294–1304 (2015).

Translated by L.Trubitsyna